Available online at www.sciencedirect.com
ScienceDirect
Nuclear Physics A 1040 (2023) 122745
NUCLEAR PHYSICS A
www.elsevier.com/locate/nuclphysa

The measurement of the half-life of the second excited state of ^{237}Np with a new detector system and digital electronics

O.C.B. Santos, J.R.B. Oliveira *, E. Macchione, R. Lichtenthäler, K.C.C. Pires, A. Lépine-Szily

Departamento de Física Nuclear, Instituto de Física, Universidade de São Paulo, 05508-090, São Paulo, Brazil

Received 1 May 2023; received in revised form 29 July 2023; accepted 8 August 2023
Available online 23 August 2023

Abstract

The half-life of the second excited state ($5/2^-$ at 59.54 keV) of ^{237}Np was measured with high precision and reliability using the coincidence method with fast scintillators and a fully digital-based electronic data acquisition system. The alpha particle from an ^{241}Am source was measured in coincidence with the gamma rays emitted by the daughter ^{237}Np nucleus. This measurement also illustrates the use of new LYSO(Ce) scintillators in particle-gamma experiments.

Keywords: Particle-gamma coincidence; LYSO(Ce) scintillator; ^{241}Am decay

1. Introduction

The alpha decay scheme of ^{241}Am nucleus is very well known [1], and calibration sources with this radioactive isotope are widespread in nuclear physics laboratories. They represent a good resource for testing radiation detector systems. In particular, they can be used to verify the absolute calibration, and the integral and differential non linearity of time measuring systems [2] in particle-gamma coincidence experiments. For such application, it is interesting to know

* Corresponding author.
E-mail address: zero@if.usp.br (J.R.B. Oliveira).

https://doi.org/10.1016/j.nuclphysa.2023.122745
0375-9474/

with as much precision and accuracy as possible the half-life of the 2nd excited state of ^{237}Np nucleus, the daughter of ^{241}Am alpha decay, which is an isomer with several tens of ns lifetime. This state decays by emission of γ-rays. It is strongly populated directly (84.8%) by the alpha decay with $E_\alpha = 5.86$ MeV, and indirectly (nearly 15%) from upper lying short lived levels through highly electronic converted transitions. The half-life of this state has been evaluated to be $t_{\frac{1}{2}} = 67.2(4)$ ns [1,3] from a weighted average of the results of experiments published from 1952 to 1972. A rather recent publication [4], focused on the illustration of the coincidence technique with the employment of low cost equipment for didactic purposes, has reported the value of $t_{\frac{1}{2}} = 67.7(1)$ ns.

The LAFN ("Laboratório Aberto de Física Nuclear", IFUSP) has recently acquired new digitizers, and LYSO(Ce) scintillator crystals which will constitute a high photopeak efficiency gamma spectrometer. This spectrometer will be capable to operate under high neutron radiation and high magnetic field environments such as that of the RIBRAS [5–7] facility (LAFN) for radioactive beam production. The first detectors of the gamma array have been assembled and their performance, together with the new digitizers, is being tested. Since LYSO(Ce) crystals present high intrinsic background due to the beta decay of one of its constituents, its performance as a γ-ray detector for nuclear physics research could be questioned. This presents one of these tests, in which the aforementioned isomeric state lifetime was measured with very good precision and reliability. At the same time, the test shows that those γ-ray detectors can indeed be used in high accuracy experiments, when good timing resolution coincidence measurements are performed with an ancillary detection system with high selectivity.

2. Experimental description

The experiment was carried out using a thin planar radioactive ^{241}Am source. The ^{237}Np second excited state ($5/2^-$ at 59.54 keV) decays directly to the ground state by an E1 transition with an electronic conversion coefficient of $\alpha_{ce} = 0.53$, or to the 1st excited state ($7/2^+$ at 33.2 keV) by a 26.3 keV highly converted gamma transition ($\alpha_{ce} = 4.4$), followed by a short lived M1+E2 transition to the ground state.

The experimental setup consisted of a 16.6×16.6 mm^2 plastic *phoswich* scintillator detector (0.1 mm thick BC-400, 2.4 ns decay time, heat-pressed in vacuum [8] to 10 mm thick BC-444, 264 ns decay time), coupled to a 4×4 Silicon Photomultiplier (SiPM, Sensl, ARRAYC-30035-16P-PCB), for charged particles, and 9 LYSO(Ce) scintillator detectors ($12.4 \times 12.4 \times 40$ mm^3 crystals), coupled to 2×2 pixel Silicon Photomultipliers (Sensl, ARRAYJ-60035-4P-BGA), for γ-rays, in a compact arrangement (see Fig. 1). The pixelated SiPM of the particle detector allows for position sensitivity in two dimensions, but this feature was not used in this experiment. The signals from the 16 pixels of the particle detector were individually amplified (by a factor of 10) by a 16 channel Phillips Scientific photomultiplier amplifier (model 776) and then summed up with linear fan-in/fan-out modules. The risetime of the pulse is about 13 ns. The signal from the 4 pixels of the gamma scintillator photomultipliers were wired in parallel in the front end electronics, designed in house. In this case the pulse risetime was about 40 ns.

The alpha source was deposited around the center of a 9.5 mm diameter well in a 16.7 mm diameter stainless steel disk, and was placed near the focus of the detectors, at about 8 mm distance from the particle detector, and 4-5 cm from the γ-ray detectors, in ambient air. The energy loss of the alpha particles in air was relatively small, so that nearly 100% of the particle signals were above the particle detection threshold. The alpha particle count rate of the detector was about 130/s during the measurements. The alpha particle support diameter frame covered

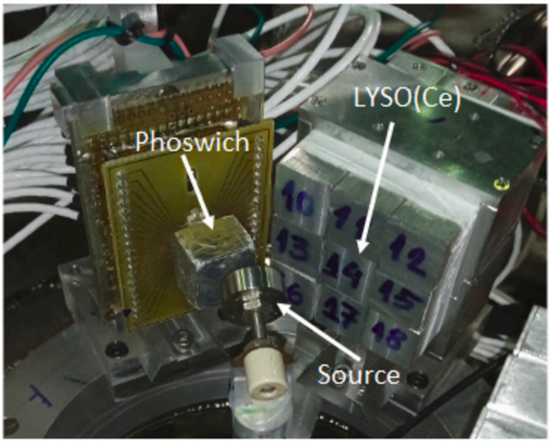

Fig. 1. Experimental setup scheme showing the α source, the plastic scintillator detector and the LYSO(Ce) γ-ray detectors.

the view of 3 of the 9 γ-ray detectors, absorbing the low energy γ-rays, and there was a bad contact in the printed circuit electronics of one detector, so that in this experiment only the other 5 LYSO(Ce) detectors were used.

To perform the experiment, a recently acquired CAEN digital pulse processing electronic module V1725, 250 MS/s, with DPP-PSD firmware [9], was used with the CoMPASS data acquisition program. The CH_0 channel was used to measure the α-particles while the $CH_{2,3,4,5,6}$ channels were used to measure the γ-ray emission from the decay of the ^{237}Np nucleus. The Constant Fraction Discriminator (CFD) technique was used to determine the arrival time of each detector signal. To determine the time, a linear interpolation was performed in the CFD signal considering two points, the first one before and the last one after the mid-scale. The time is determined considering the crossover between the interpolation and the mid-scale (zero crossing), and saved with a precision of 4 ps on the Time Stamp parameter value of the digitizer. For more details see the CoMPASS user manual [10].

The gamma detector data was registered only if the absolute time difference to the charged particle signal was within 1500 ns. LYSO(Ce) detectors present a significant intrinsic radiation [11,12], originated from the ^{176}Lu naturally occurring isotope beta decay. Nevertheless, the fast timing coincidence with the particle detector allows for a very effective filtering of these uncorrelated gamma events, as it will be shown.

Fig. 2 shows a two dimensional energy spectrum Eα-Eγ obtained in the coincidence measurements, within the full time range (-1.5 μs to 1.5 μs). The vertical axis shows the α-particle energies, while the horizontal axis shows the γ-ray energies emitted by both, the ^{241}Am radioactive source (time correlated) and the intrinsic radiation of LYSO(Ce) detectors (uncorrelated). The vertical axis is in channels and the horizontal axis was calibrated in energy (keV). This calibration was performed using the escape γ-rays with energies 202 and 307 keV emitted by LYSO detectors [12], and the γ-ray of 59.54 keV emitted by the ^{237}Np nucleus.

The acquisition system PSD firmware allows to define two integration gates: a short-gate and a long-gate. Using the short-gate range (20 ns for the particle pulse and 80 ns for the gamma pulse, counting from the beginning of the pulses) it is possible to integrate part of the pulse corresponding to a part of the energy of the detected particle (ΔE) and using the long-gate range (160 ns for alpha and 450 ns for gamma), the full pulse could be integrated corresponding to

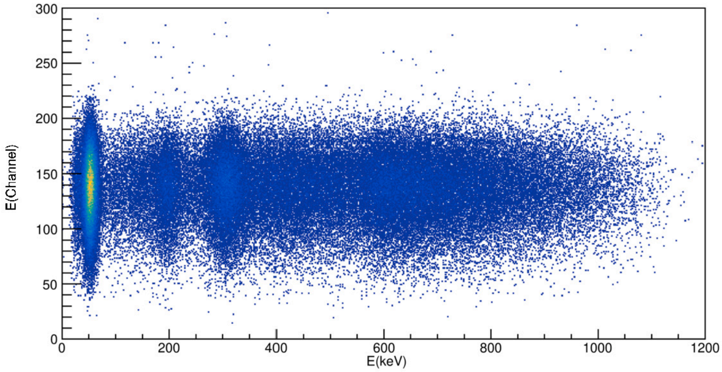

Fig. 2. Two dimensional energy spectrum of α-γ coincidence measurements. Vertical axis α-particle energy, in channels, and horizontal axis γ-ray energy, in keV.

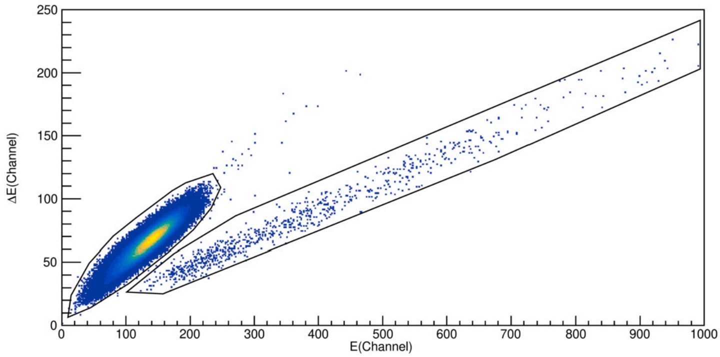

Fig. 3. Two dimensional spectrum ΔE-E of the particle detector in coincidence with the gamma detectors. The alpha (left) and electron (right) cut regions are shown.

the total energy of the detected particle (E). In the present case, the full energy of the alpha particles from the ^{241}Am decays is deposited in the 0.1 mm fast scintillator layer of the plastic *phoswich* detector. Fig. 3 presents the ΔE-E charged particle spectrum in coincidence with gamma rays. The well defined peak delimited by a graphical cut on the left is associated with the α-particles. Electrons from Compton and Photoelectric effect (*e.g.* from the gamma escape radiation of LYSO(Ce) ^{176}Lu decay) which interact mostly with the 1 cm thick slow scintillator bulk, only. A significant part of the slow scintillator pulse is integrated in the short gate. A graphical cut of these electron-related events, extending to channel 1000 in E, is also shown. Note that, besides the conversion factor from energy loss to scintillation being different for different particle types, the E detector has a larger scintillation yield than the ΔE.

Fig. 4 shows the projection of the α-γ two dimensional spectrum (Fig. 2) on the γ energy axis, expanded around the main coincidence peak. Fig. 4 shows two peaks: the most intense peak is related to the gamma decay from the 2nd excited state to the gs of the ^{237}Np and the small peak to the gamma decays from the 2nd to the 1st excited state and from the 1st to the gs of ^{237}Np.

Fig. 5 shows the time difference $\Delta t = t_\gamma - t_\alpha$ spectra between gamma and alpha particle times considering all events in Fig. 2.

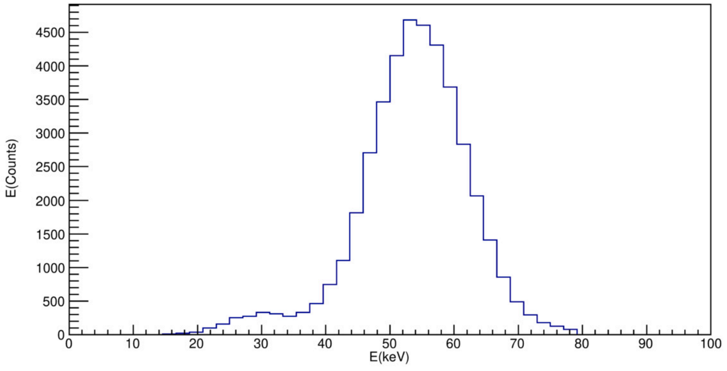

Fig. 4. α-γ coincidence peak projection on the gamma energy axis.

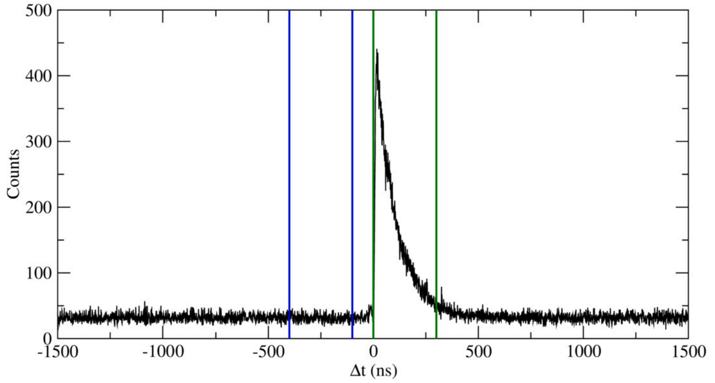

Fig. 5. Time difference spectrum between gamma rays and alpha particles. The uncorrelated background (left) and correlated peak (right) cut regions are shown (see text).

Fig. 6 shows the projection on the gamma energy axis of the time cuts (green, at right, and blue, at left) presented in the time spectrum Fig. 5. It illustrates that the intrinsic radioactivity of LYSO(Ce), which is uncorrelated with the alpha particles and dominates the spectrum above 100 keV, contributes very little to spectrum below this energy, where the alpha-correlated gamma events appear. This means that the possibility of any contamination by a spurious line is kept at a minimum, and the measurement statistics uncertainties prevail. In addition, the high precision and accuracy of the fast digitizer electronics avoids any relevant systematic errors associated with the time calibration.

The α-γ time difference spectrum with energy gate on the peaks shown in Fig. 4, originated from the decay of the 2$^{\text{nd}}$ excited state of ^{237}Np, is shown in Fig. 7.

3. Analysis

The time difference spectra between the α-particle, emitted by ^{241}Am source, and the γ-ray, emitted by the decay of the second excited state of ^{237}Np nucleus, are well described by exponential functions. The adjustments carried out to obtain the half-life ($t_{\frac{1}{2}}$) of the second excited state of ^{237}Np nucleus were based on the following model:

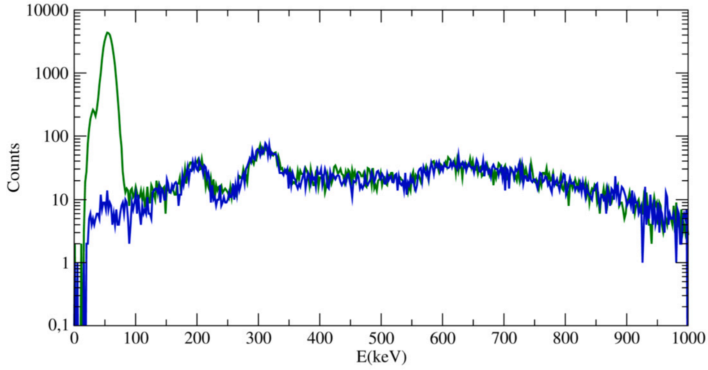

Fig. 6. Gamma-ray energy histograms of the time cuts presented in Fig. 5 (left cut, in blue, and right cut, in green). (For interpretation of the colors in the figure(s), the reader is referred to the web version of this article.)

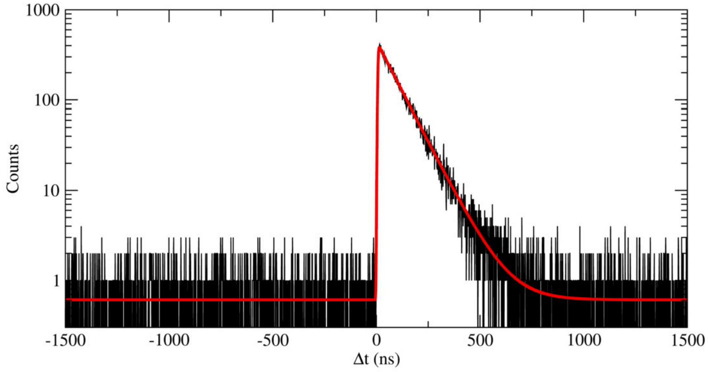

Fig. 7. The α-γ time difference spectrum gated by the gamma energy peaks of Fig. 4 (E < 78 keV). The black line histogram is the data and the continuous red line is the fit.

$$f(t;\tau,T_0,A,B)=\begin{cases} B, & \text{if } t<T_0 \\ B+A*\exp\left[-\frac{t-T_0}{\tau}\right], & \text{if } t>T_0 \end{cases} \tag{1}$$

where $t_{\frac{1}{2}}=\tau\ln[2]$, B is the background constant and A is the amplitude of the exponential when $T=T_0$.

To take into account the time resolution, a Gaussian convolution was considered in equation (1) (see equation (2)), where σ is the resolution time and G is a Gaussian function.

$$\eta(t;\tau,T_0,A,B,\sigma)=\int_{-\infty}^{\infty} f(x)G[(t-x),\sigma]dx \tag{2}$$

The time difference spectra for each γ detector were adjusted by using the equation (2) and one fit is presented in Fig. 7. The other fits are similar.

The Table 1 shows the parameters obtained for all fits.

The weighted average obtained using the half-live ($t_{\frac{1}{2}}$) values presented in Table 1 is $t_{\frac{1}{2}}$=67.60(20) ns. This value is compatible with National Nuclear Data Center (NNDC) evalu-

Table 1
Parameters obtained by fitting of the time difference spectra between α-γ coincidence measurements for each LYSO(Ce) γ-ray detector.

A	B	T_0 (ns)	$t_{\frac{1}{2}}$ (ns)	σ (ns)	χ^2_{red}
414.9(30)	0.609(16)	7.48(12)	67.30(37)	3.11(11)	1.02
254.1(24)	0.550(15)	8.67(16)	67.8(5)	3.32(15)	1.04
122.4(17)	0.575(16)	-4.67(22)	68.5(7)	3.15(21)	0.98
239.7(23)	0.738(18)	7.20(15)	67.5(5)	3.09(15)	1.02
362.4(28)	0.412(13)	-0.18(13)	67.68(39)	3.47(12)	0.99

ation [1], based on Refs. [13–17] (67.2(7) ns) and very close to the value obtained in Ref. [4] (67.7(1) ns) with a FPGA-based didactic laboratory equipment.

4. Summary and conclusions

The half-life of the second excited state ($5/2^-$ at 59.54 keV) of ^{237}Np was measured and the obtained value is $t_{\frac{1}{2}}$=67.60(20) ns. This value is consistent with previous data from the literature [4,13–17] and presents a smaller uncertainty than the weighted average value [3], from data with 0.7 ns uncertainty or larger. The experiment demonstrates the feasibility of high precision and reliability particle-gamma coincidence measurements with fast scintillators, including LYSO(Ce) γ-ray detectors, and fast digital electronics.

CRediT authorship contribution statement

O.C.B. Santos: Conceptualization, Data curation, Investigation, Methodology, Software, Writing – original draft, Writing – review & editing. **J.R.B. Oliveira:** Conceptualization, Investigation, Methodology, Software, Supervision, Writing – original draft, Writing – review & editing. **E. Macchione:** Investigation, Methodology. **R. Lichtenthäler:** Conceptualization, Supervision, Writing – review & editing. **K.C.C. Pires:** Investigation, Writing – review & editing. **A. Lépine-Szily:** Funding acquisition, Project administration, Supervision, Writing – review & editing.

Declaration of competing interest

The authors declare that they have no known competing financial interests or personal relationships that could have appeared to influence the work reported in this paper.

Data availability

Data will be made available on request.

Acknowledgements

This work has been partially supported by Fundação de Amparo à Pesquisa do Estado de São Paulo, Brazil (FAPESP) - contracts ns. 2016/04612-9, 2019/07767-1, 2019/02759-0 and 2021/12254-3 (OCBS); Conselho Nacional de Desenvolvimento Científico e Tecnológico, Brazil

(CNPq) project no. 405138/2021-0, and 316019/2021-6 (JRBO) and INCT-FNA project no. 464898/2014-5.

References

[1] M. Basunia, Nuclear data sheets for a = 237, Nucl. Data Sheets 107 (8) (2006) 2323–2422, https://doi.org/10.1016/j.nds.2006.07.001.

[2] G. Miller, P. Dillard, M. Eckhause, R. Welsh, Determinations of nuclear level halflives in ^{85}Rb and ^{237}Np and their use as timing standards, Nucl. Instrum. Methods 104 (1) (1972) 11–12, https://doi.org/10.1016/0029-554X(72)90290-X.

[3] BNL National Nuclear Data Center, Nudat (nuclear structure and decay data), https://www.nndc.bnl.gov/. (Accessed 15 April 2023).

[4] M. Vretenar, N. sa Erceg, M. Karuza, Energy-resolved coincidence counting using an FPGA for nuclear lifetime experiments, Am. J. Phys. 87 (2019) 997, https://doi.org/10.1119/1.5122744.

[5] R. Lichtenthäler, A. Lépine-Szily, V. Guimarães, C. Perego, V. Placco, O. Camargo Jr., R. Denke, P.N. de Faria, E.A. Benjamim, N. Added, G.F. Lima, M.S. Hussein, J. Kolata, A. Arazi, Radioactive ion beams in Brazil (RIBRAS), Eur. Phys. J. A 25 (2005) 733, https://doi.org/10.1140/epjad/i2005-06-043-y.

[6] A. Lépine-Szily, R. Lichtenthäler, V. Guimarães, The radioactive ion beams in Brazil (RIBRAS) facility, Eur. Phys. J. A 50 (2014) 128, https://doi.org/10.1140/epja/i2014-14128-4.

[7] R. Lichtenthäler, O.C.B. Santos, A. Serra, U. Umbelino, K.C.C. Pires, J.R.B. Oliveira, A. Lépine-Szily, P.N. de Faria, V. Morcelle, Experiments with A = 6-8 exotic beams in RIBRAS, Eur. Phys. J. A 57 (2021) 92, https://doi.org/10.1140/epja/s10050-021-00411-0.

[8] J. Alcántara-Núñez, J. Oliveira, E. Cybulska, N. Medina, M. Rao, R. Ribas, M. Rizzutto, W. Seale, F. Falla-Sotelo, F. Espinoza-Quiñones, C. Tenreiro, SACI-a 4π plastic phoswich array ancillary detector system of a γ-ray spectrometer, Nucl. Instrum. Methods Phys. Res., Sect. A, Accel. Spectrom. Detect. Assoc. Equip. 497 (2) (2003) 429–439, https://doi.org/10.1016/S0168-9002(02)01926-5.

[9] CAEN, V1725/v1725s 16/8 channel 14-bit 250 ms/s digitizer, https://www.caen.it/products/v1725/, 2023. (Accessed March 2023).

[10] CAEN Spa, UM5960 CoMPASS user manual, https://www.caen.it/download/?filter=CoMPASS. (Accessed April 2023).

[11] I. Mouhti, A. Elanique, M. Messous, A. Benahmed, J. McFee, Y. Elgoub, P. Griffith, Characterization of CsI(Tl) and LYSO(Ce) scintillator detectors by measurements and Monte Carlo simulations, Appl. Radiat. Isot. 154 (2019) 108878, https://doi.org/10.1016/j.apradiso.2019.108878.

[12] F.E. Enríquez-Mier-y-Terán, A.S. Ortega-Galindo, T. Murrieta-Rodríguez, M. Rodríguez-Villafuerte, A. Martínez-Dávalos, H. Alva-Sánchez, Coincidence energy spectra due to the intrinsic radioactivity of LYSO scintillation crystals, EJNMMI Phys. 7 (21) (2020), https://doi.org/10.1186/s40658-020-00291-1.

[13] E. Sakai, H. Tamura, Y. Sarurai, Absolute measurements of the disintegration rates of americium-241 sources by using semiconductor detectors, J. Nucl. Sci. Technol. 1 (3) (1964) 101–107, https://doi.org/10.1080/18811248.1964.9732088.

[14] J.K. Beling, J.O. Newton, B. Rose, The decay of Am^{241}, Phys. Rev. 87 (1952) 670–671, https://doi.org/10.1103/PhysRev.87.670.

[15] E.S. Oberhofer, An investigation of isomeric transitions following the decay of ^{237}Np, ^{241}Am, and ^{243}Am, Ph.D. thesis, North Carolina State University, 1968.

[16] J. Turner, LXXIX. The internal conversion electron spectrum of ^{241}Am, Lond. Edinb. Dublin Philos. Mag. J. Sci. 46 (378) (1955) 687–700, https://doi.org/10.1080/14786440708520596.

[17] R.K. Garg, S.D. Chauhan, S.L. Gupta, N.K. Saha, Half-life measurements of the 86.6 keV level in ^{233}Pa and 59.6 keV level in ^{237}Np, Z. Phys. A, Hadrons Nucl. 244 (1971) 312–320, https://doi.org/10.1007/BF01396790.